J. Fluid Mech. (1994), *vol.* 259, *pp.* 241–264

Stretched vortices – the sinews of turbulence; large-Reynolds-number asymptotics

By H. K. MOFFATT[1], S. KIDA[2] AND K. OHKITANI[2]

[1] Department of Applied Mathematics and Theoretical Physics, University of Cambridge, Silver Street, Cambridge CB3 9EW, UK

[2] Research Institute for Mathematical Sciences, Kyoto University, Kyoto 606-01, Japan

(Received 22 April 1993)

A large-Reynolds-number asymptotic theory is presented for the problem of a vortex tube of finite circulation Γ subjected to uniform non-axisymmetric irrotational strain, and aligned along an axis of positive rate of strain. It is shown that at leading order the vorticity field is determined by a solvability condition at first-order in $\epsilon = 1/R_\Gamma$ where $R_\Gamma = \Gamma/\nu$. The first-order problem is solved completely, and contours of constant rate of energy dissipation are obtained and compared with the family of contour maps obtained in a previous numerical study of the problem. It is found that the region of large dissipation does not overlap the region of large enstrophy; in fact, the dissipation rate is maximal at a distance from the vortex axis at which the enstrophy has fallen to only 2.8% of its maximum value. The correlation between enstrophy and dissipation fields is found to be $0.19 + O(\epsilon^2)$. The solution reveals that the stretched vortex can survive for a long time even when two of the principal rates of strain are positive, provided R_Γ is large enough. The manner in which the theory may be extended to higher orders in ϵ is indicated. The results are discussed in relation to the high-vorticity regions (here described as 'sinews') observed in many direct numerical simulations of turbulence.

1. Introduction

One of the most striking features of the structure of turbulence observed in many numerical simulations (Siggia 1981; Kerr 1985; Hosokawa & Yamamoto 1989, 1990; She, Jackson & Orszag 1990; Ruetsch & Maxey 1991; Vincent & Meneguzzi 1991; Douady, Couder & Brachet 1991; Kida & Ohkitani 1992; Jiménez *et al.* 1993; Kida 1993) is the emergence of high-vorticity regions concentrated in tube-like structures which occupy a relatively small fraction ($\sim 1\%$) of the total volume, but which account for a much larger fraction (typically 10–20%) of the viscous dissipation of turbulent energy (Hosokawa & Yamamoto 1989).† The tubes have a length of the order of the integral scale of the turbulence, and a cross-sectional radius somewhere between the inner Kolmogorov scale and the Taylor microscale (Tennekes 1968; Vincent & Meneguzzi 1991), and are generally interpreted as vortex tubes which are stretched and concentrated, in a manner analogous to the familiar Burgers vortex, by the local straining associated with the turbulence field. The radius of the Burgers vortex subjected to a stretching rate γ is $\delta \sim (\nu/\gamma)^{\frac{1}{2}}$, and if γ is a typical turbulence strain rate, then δ is of the order of the inner Kolmogorov scale.

† These percentages depend on the threshold that is used to define 'high vorticity'. If this threshold is lowered, then both the volume fraction and the fraction of dissipation increase.

Vortices have been described as the 'sinews' of fluid motion (Küchemann 1965; Saffman & Baker 1979), a term that now seems particularly apt for the above concentrated vortex tubes. Just as sinews serve to connect a muscle with a bone or other structure, so the concentrated vortices of turbulence serve to connect large eddies of much weaker vorticity; and just as sinews can take the stress and strain of muscular effort, so the concentrated vortices can accommodate the stress associated with the low pressure in their cores and the strain imposed by relative motion of the eddies into which they must merge at their ends. Thus the term 'sinews of turbulence' seems well-chosen to describe these high vorticity regions;† hence the title of this paper.

The idea that the dissipative structures of turbulence may be well represented by a random distribution of strained vortex sheets or tubes goes back to Townsend (1951) (see the discussion in Batchelor 1953, §7.4). Suppose that the background straining flow has the form

$$U = (\alpha x, \beta y, \gamma z), \tag{1.1}$$

where

$$\alpha+\beta+\gamma = 0, \qquad \alpha < 0 \leqslant \gamma, \quad \beta \geqslant \alpha. \tag{1.2}$$

If $\beta < 0$, then there is *one positive* principal rate of strain (γ), and there is a tendency to form vortex tubes aligned with the corresponding axis of strain (Oz); we shall describe this type of strain as *axial strain*. If $\beta > 0$, then there are *two positive* principal rates of strain (β and γ), and there is a tendency to form vortex sheets in the plane of the corresponding axes of strain (Oy, Oz); we shall describe this type of strain as *biaxial strain*. If $\beta = 0$ and $\alpha = -\gamma$, then of course we have the case of *plane strain*. We may characterize the different types of strain by the single strain parameter

$$\lambda = \frac{\alpha-\beta}{\alpha+\beta} \quad (\lambda \geqslant 0) \tag{1.3}$$

as follows:

$\lambda = 0,$	axisymmetric axial strain;
$0 < \lambda < 1,$	axial strain;
$\lambda = 1,$	plane strain;
$1 < \lambda < 3,$	biaxial strain with $0 < \beta < \gamma$;
$\lambda = 3,$	axisymmetric biaxial strain ($\beta = \gamma$);
$\lambda > 3,$	biaxial strain with $\beta > \gamma$.

Note that the determinant of the rate-of-strain matrix is given by

$$\alpha\beta\gamma = \tfrac{1}{4}\gamma^3(1-\lambda^2). \tag{1.4}$$

It is well known that $\overline{\alpha\beta\gamma} < 0$, the overbar denoting the ensemble average, in homogeneous isotropic turbulence, so that there would appear to be a statistical bias towards regions of biaxial strain. However, as pointed out by Jiménez (1992) and Kida (1993), the presence of a strained vortex itself modifies the local strain field, tending to convert axial strain to biaxial strain, so that care is needed in this inference. Moreover, vortex sheets are in any case subject to Kelvin–Helmholtz instability, an instability that is modified but not completely suppressed by strain (Lin & Corcos 1984); this instability leads to spiral wind-up of a vortex sheet and to the formation of a row of parallel vortex tubes of spiral structure. Spiral structures have been considered as

† The alternative term 'worms' has been suggested by Yamamoto & Hosokawa (1988). We prefer the term 'sinews' for the reason given above, and also because vortex tubes, unlike worms, do not have clearly defined end-points.

candidates for the typical dissipative structures of turbulence (Lundgren 1982; Moffatt 1984, 1993) but clear evidence for spiral structures from direct numerical simulations (DNS) of turbulence is not yet available.

Vortex tubes formed either in regions of axial strain or (via the Kelvin–Helmholtz mechanism) in regions of biaxial strain are in general represented by fully nonlinear solutions of the Navier–Stokes equations, the nonlinearity arising through convection of the (generally non-axisymmetric) vorticity field $\boldsymbol{\omega}$ by the rotational velocity $\boldsymbol{u}$ (where $\boldsymbol{\omega} = \boldsymbol{\nabla} \times \boldsymbol{u}$). Only in the axisymmetric case ($\beta = \alpha$) is an exact solution of the Navier–Stokes equation of finite circulation available; this is the Burgers vortex for which $\boldsymbol{\omega} = (0, 0, \omega(r))$ with

$$\omega(r) = \frac{\gamma \Gamma}{4\pi\nu} \exp\left[-\frac{\gamma r^2}{4\nu}\right]. \tag{1.5}$$

Here, Γ is the total circulation associated with the vortex. If $\alpha \leqslant \beta < 0$, and if the Reynolds number

$$R_\Gamma = \Gamma/\nu \tag{1.6}$$

is very *small*, so that self-induced convection of vorticity is negligible, then the *linearized* vorticity equation admits a unique solution similar to (1.5), namely

$$\omega(x, y) = \frac{(\alpha\beta)^{\frac{1}{2}}\Gamma}{2\pi\nu} \exp\left[\frac{\alpha x^2 + \beta y^2}{2\nu}\right], \tag{1.7}$$

so that iso-vorticity contours $\omega = \text{const.}$ are ellipses with principal axes aligned with the principal axes of strain (see Appendix A).

Study of the effects of nonlinearity for larger R_Γ was initiated by Robinson & Saffman (1984) (see also Saffman 1992, §13.3), who developed a double series solution in terms of the Reynolds number (still assumed small) and the strain parameter λ, representing the departure from axisymmetry in the imposed strain field (1.1), and also assumed small; they also provided numerical evidence for the continued existence of such vortices for Reynolds number up to 100 and values of λ up to 0.75. In turbulence, we are particularly interested in *large* values of R_Γ (Jiménez *et al.* 1993 provide evidence for a scaling law $R_\Gamma \sim Re^{\frac{1}{2}}$ where Re is the turbulent Reynolds number based on the Taylor microscale) and also in the full range of values of λ, not only the range $0 \leqslant \lambda \leqslant 1$, but also the range $\lambda > 1$ (i.e. $\beta > 0$) since, as will emerge, strong vortex tubes can survive for a very long time even in regions of biaxial strain (see §5).

Renewed interest in this problem has been kindled by two numerical studies: first that of Buntine & Pullin (1989) who studied the time-dependent merger of two vortices in a strain field with $\lambda = \frac{1}{2}$ and $R_\Gamma/2\pi$ in the range 10 to 1280; and second, that of Kida & Ohkitani (1992, hereafter referred to as KO92) who (in the Appendix to their paper) analysed the stretched vortex problem numerically and computed not only steady iso-vorticity contours for $\lambda = \frac{1}{2}$ and a range of values of R_Γ up to 500, but also the contours of constant energy dissipation rate $\Phi = 2\nu s_{ij} s_{ij}$, where s_{ij} is the rate-of-strain tensor (including both the background strain field and the contribution from the vortex). KO92 showed that (i) the principal axes of the contours $\omega = \text{const.}$ rotate anticlockwise towards the lines $x = \pm y$ at 45° to the axes of strain Ox, Oy as R_Γ increases, and at the same time tend to become more circular in form; (ii) the contours of the dissipation function Φ evolve in a rather complex manner as R_Γ increases, but the function always exhibits two maxima on or near the line $x = -y$ and symmetrically displaced from the vortex centre. A similar double-peaked structure of the dissipation function was noted in the high-vorticity regions (sinews) of a DNS at Reynolds number (based on the

Taylor microscale) $Re \approx 186$ (KO92, figure 6*b*); in this numerical experiment, concentrated vortices with values of R_Γ in the range 50–100 were observed.

It is obviously important to understand the reasons for the changing structure of both vorticity and dissipation fields as R_Γ increases, and this is the aim of the present paper. We approach the problem as one in high-Reynolds-number asymptotics. At leading order, the iso-vorticity lines are circular; the distribution of ω as a function of radius r is not determined at this order, but is determined by a solvability condition at the next order of approximation. The same phenomenon was encountered by Neu (1984) in a study of the unsteady dynamics of vortices subjected to plane strain (the case $\lambda = 1$ in our notation). Here we solve the problem fully to order $\epsilon = 1/R_\Gamma$, at which level the results depend on ϵ and λ only through the combination $\epsilon_1 = \epsilon\lambda$. We present the asymptotic form of the vorticity field to this order in §2, and in §3 we analyse the structure of the dissipation field Φ. There are indeed interesting, but fully comprehensible, changes in the structure of this function as revealed by a study of its saddle points and their connections. The results are fully compatible with those of KO92, and permit confident application of the asymptotic theory for all values of λ, and for arbitrarily large R_Γ. In §4, we extend the theory to the next level of approximation, $O(\epsilon^2)$, and indicate the procedure for extension to still higher order (the solvability condition at order ϵ^3 is obtained in Appendix B). In §5, we consider particular problems that arise when $\lambda > 1$. Finally, in §6, we assess the significance of the results in the framework of high-Reynolds-number turbulence.

2. Stretched vortex: asymptotic solution for $R_\Gamma \gg 1$

Let $u_x(=\partial\psi/\partial y)$ and $u_y(=-\partial\psi/\partial x)$ be the additional velocity components associated with the vortex, with vorticity

$$\omega = \frac{\partial u_y}{\partial x} - \frac{\partial u_x}{\partial y} = -\nabla^2\psi. \tag{2.1}$$

We suppose that the total circulation

$$\Gamma = \int\int \omega(x, y)\,\mathrm{d}x\,\mathrm{d}y \tag{2.2}$$

is finite, and that

$$\epsilon = 1/R_\Gamma = \nu/\Gamma \ll 1. \tag{2.3}$$

The steady vorticity equation that we wish to solve is

$$(\alpha x + u_x)\frac{\partial\omega}{\partial x} + (\beta y + u_y)\frac{\partial\omega}{\partial y} = \gamma\omega + \nu\nabla^2\omega. \tag{2.4}$$

The configuration is sketched in figure 1, for (*a*) axial and (*b*) biaxial strain regions.

Anticipating that, even when $\alpha \neq \beta$, the radial lengthscale is still of order $\delta = (\nu/\gamma)^{\frac{1}{2}}$, and the maximum velocity in the region of the vortex is of order Γ/δ, let us introduce dimensionless variables

$$(x^*, y^*) = (x, y)/\delta, \quad (\alpha^*, \beta^*) = (\alpha, \beta)/\gamma, \quad \psi^* = \psi/\Gamma. \tag{2.5}$$

Substituting in (2.4) and dropping the stars, we obtain the dimensionless equation

$$\frac{\partial(\psi, \omega)}{\partial(x, y)} = \epsilon\left[\left(\alpha x\frac{\partial}{\partial x} + \beta y\frac{\partial}{\partial y}\right)\omega - \omega - \nabla^2\omega\right]. \tag{2.6}$$

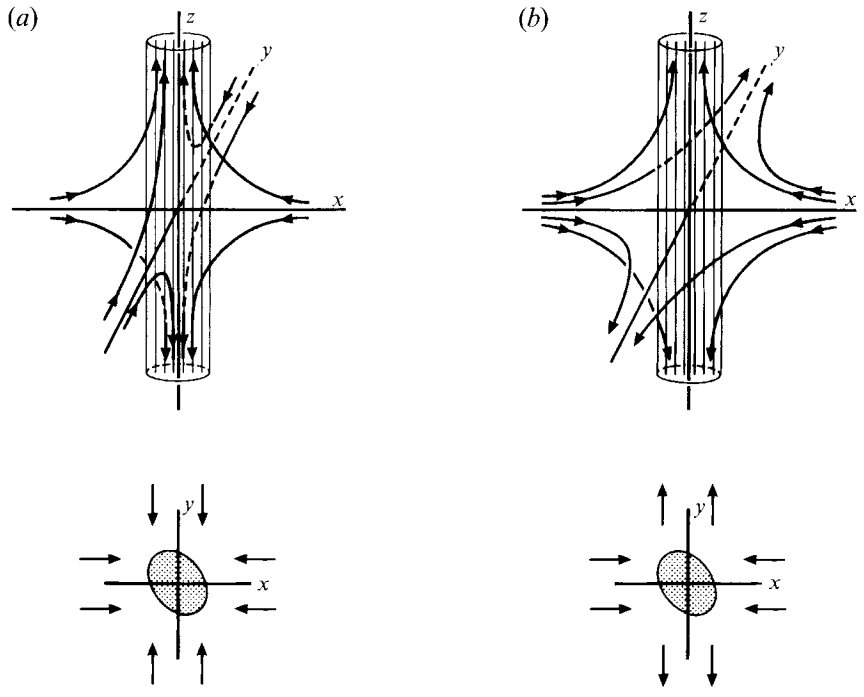

FIGURE 1. Sketch of the configuration considered. Perspective view of vortex $\boldsymbol{\omega} = (0, 0, \omega(x, y))$ stretched by the flow $\boldsymbol{U} = (\alpha x, \beta y, \gamma z)$, and (below) cross-section of the flow in the (x, y)-plane. (*a*) Axial strain. (*b*) Biaxial strain.

Note that now $\alpha + \beta = -1$ and that the third (dimensionless) strain rate is $+1$.

In the dimensionless variables adopted here, the time $t_0 = \delta^2/\Gamma$ characteristic of the circulating motion around the vortex becomes of order unity, and the time $t_\nu = \delta^2/\nu$ characteristic of viscous diffusion over a scale δ becomes of order R_Γ.

It is convenient to adopt plane polar coordinate (r, θ) with $x = r\cos\theta, y = r\sin\theta$. Then (2.6) may be transformed to

$$\frac{1}{r}\frac{\partial(\psi, \omega)}{\partial(r, \theta)} = -\epsilon \mathrm{L}_0 \omega - \epsilon\lambda \mathrm{L}_1 \omega, \tag{2.7}$$

where

$$\mathrm{L}_0 = 1 + \frac{r}{2}\frac{\partial}{\partial r} + \nabla^2, \tag{2.8}$$

$$\mathrm{L}_1 = \frac{1}{2}\left(\cos 2\theta\, r\frac{\partial}{\partial r} - \sin 2\theta \frac{\partial}{\partial \theta}\right), \tag{2.9}$$

and where now $\lambda = \beta - \alpha$, so that

$$\alpha = -\tfrac{1}{2}(1+\lambda), \quad \beta = -\tfrac{1}{2}(1-\lambda). \tag{2.10}$$

This form of the equations proves most convenient for subsequent analysis.

We seek a solution of (2.7) in the form

$$\psi = \psi_0 + \epsilon\psi_1 + \epsilon^2\psi_2 + \ldots, \tag{2.11}$$

with corresponding expansions for the velocity components

$$u = \frac{1}{r}\frac{\partial\psi}{\partial\theta}, \quad v = -\frac{\partial\psi}{\partial r}, \tag{2.12}$$

and for the vorticity

$$\omega = -\nabla^2\psi = -\left(\frac{1}{r}\frac{\partial}{\partial r}r\frac{\partial}{\partial r}+\frac{1}{r^2}\frac{\partial^2}{\partial\theta^2}\right)\psi. \tag{2.13}$$

At order ϵ^0, we obtain the Euler equation

$$\frac{\partial(\psi_0,\omega_0)}{\partial(r,\theta)} = 0, \tag{2.14}$$

so that $\omega_0 = \mathscr{F}(\psi_0)$ for some function $\mathscr{F}$. If we assume that the flow ψ_0 has a single stagnation point at $r = 0$, the streamlines being closed curves around this stagnation point, then it seems highly probable that the only solutions of (2.14) in an unbounded fluid and with localized vorticity are of the form $\psi_0 = \psi_0(r)$, i.e. the streamlines (and so the iso-vorticity lines also) are circles $r = \text{const}$. Certainly this is consistent with the trend noted by KO92. We note moreover that it has been recently shown by Linardatos (1993) that in the closely related problem of finding magnetic equilibria in a perfectly conducting fluid by the method of magnetic relaxation (Moffatt 1985), the minimum-energy states with a single null-point do indeed have circular field lines.

At any rate, we shall restrict attention to this class of solutions of (2.14), i.e. we assume $\psi_0 = \psi_0(r)$ so that

$$\omega_0(r) = -\psi_0'' - r^{-1}\psi_0', \tag{2.15}$$

and the associated velocity components are

$$u_0 = 0, \quad v_0 = -\psi_0'. \tag{2.16}$$

Here, and subsequently, the prime is used to denote differentiation with respect to r. The function $\psi_0(r)$ is not determined at this level of approximation.

Now equating terms of order ϵ in (2.7), we obtain

$$-\frac{1}{r}\left[\frac{\partial(\psi_1,\omega_0)}{\partial(r,\theta)}+\frac{\partial(\psi_0,\omega_1)}{\partial(r,\theta)}\right] = \frac{1}{r}\frac{\partial}{\partial\theta}(\omega_0'\psi_1+v_0\omega_1) = \mathrm{L}_0\omega_0+\lambda\mathrm{L}_1\omega_0. \tag{2.17}$$

Averaging over θ, we obtain the solvability condition

$$\mathrm{L}_0\omega_0 = 0, \tag{2.18}$$

and this has solution, finite at $r = 0$ and vanishing at $r = \infty$,

$$\omega_0(r) = \frac{1}{4\pi}\mathrm{e}^{-r^2/4}, \tag{2.19}$$

where we have normalized so that the total (dimensionless) vortex strength is unity (consistent with the dimensional constraint (2.2)). Thus, despite the non-axisymmetry of the strain ($\lambda > 0$), the vorticity field at leading order is precisely that of the axisymmetric Burgers vortex and is independent of the strain parameter λ. This remarkable result has already been obtained by Neu (1984) for the particular case of plane strain ($\lambda = 1$). The result is quite subtle because it means that viscosity has an important residual effect even in the limit of infinite Reynolds number. In this respect, the result (2.19) is reminiscent of the Prandtl–Batchelor theorem (Batchelor 1956) for two-dimensional steady flow with closed streamlines, which establishes a similar residual effect of viscosity (in establishing a uniform vorticity distribution outside boundary layers) in the limit $\nu \to 0$. By analogy with that situation, we may conjecture that it will take a time of order $R_\Gamma^{\frac{1}{3}}$ to establish the steady state (2.19) starting from an initial condition in which ω is localized within an area of order unity but otherwise

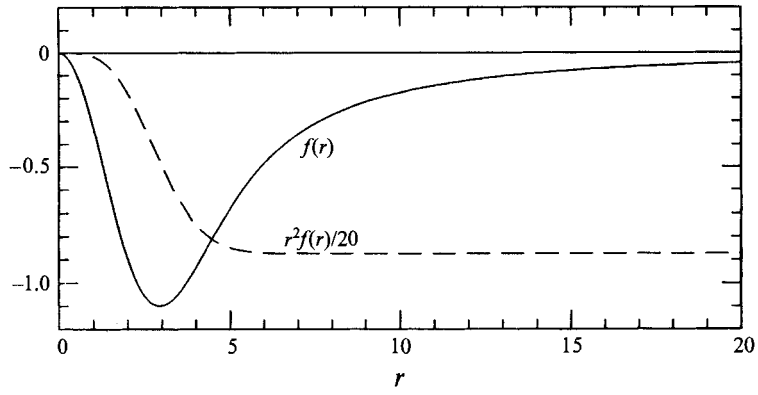

FIGURE 2. The function $f(r)$ determined by (2.25), (2.28) and (2.29). The dashed curve shows the required convergence of $r^2 f(r)$ to a constant as $r \to \infty$.

arbitrary (Rhines & Young 1982). (A residual disturbance approximately constant on streamlines $\psi = \text{const.}$ may persist on the longer timescale $O(R_\Gamma)$; the time-dependent problem (cf. Buntine & Pullin 1989) deserves further study in this respect.) Note that the circulatory velocity corresponding to (2.19) is

$$v_0(r) = \frac{1}{2\pi r}(1 - e^{-r^2/4}), \tag{2.20}$$

and the streamfunction is

$$\psi_0(r) = -\frac{1}{2\pi}\int_0^r (1 - e^{-r'^2/4})\, r'^{-1}\, dr'. \tag{2.21}$$

Returning now to (2.17), and using (2.18), we have

$$\frac{1}{r}\frac{\partial}{\partial\theta}(\omega_0' \psi_1 + v_0 \omega_1) = \lambda L_1 \omega_0 = \tfrac{1}{2}\lambda r \omega_0' \cos 2\theta. \tag{2.22}$$

Hence,

$$v_0 \nabla^2 \psi_1 - \omega_0' \psi_1 = -\tfrac{1}{4}\lambda r^2 \omega_0' \sin 2\theta + q(r), \tag{2.23}$$

for some function $q(r)$. Hence we may set

$$\psi_1 = \lambda f(r) \sin 2\theta + g(r), \tag{2.24}$$

where

$$f'' + r^{-1} f' - 4r^{-2} f = (f - \tfrac{1}{4}r^2)\,\eta(r) \tag{2.25}$$

with

$$\eta(r) = \frac{\omega_0'}{v_0} = -\frac{r^2}{4(e^{r^2/4} - 1)}. \tag{2.26}$$

The function $g(r)$ is not determined at this level, but will be shown to be zero (see the final paragraph of this section) on the basis of a solvability condition at order ϵ^2.

For small r, $\eta(r)$ has the Taylor expansion

$$\eta(r) = -1 + \tfrac{1}{8}r^2 - \tfrac{1}{192}r^4 + \ldots, \tag{2.27}$$

and, by elementary techniques, the expansion for $f(r)$ may be found in the form

$$f(r) = ar^2 + \tfrac{1}{12}(\tfrac{1}{4} - a)(r^4 - \tfrac{5}{64}r^6 + \ldots), \tag{2.28}$$

where the constant a is to be determined in such a way that the outer boundary condition

$$r^2 f(r) \to C \quad \text{as} \quad r \to \infty \tag{2.29}$$

is satisfied (ensuring that the flow is irrotational as $r \to \infty$). Numerical solution of (2.25) determines $f(r)$ (see figure 2), and the constants a and C:

$$a = -0.381475\ldots, \quad C = -17.4723\ldots. \tag{2.30}$$

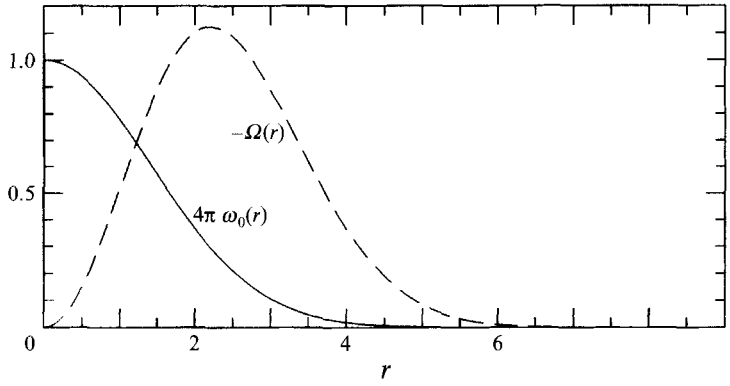

FIGURE 3. The vorticity functions $4\pi\omega_0(r)$ (solid line), $-\Omega(r)$ (dashed line) defined by (2.19) and (2.34).

Note that $f(r) < 0$ for all $r > 0$, and that $f(r)$ has a single well-defined minimum at $r = r_1 \approx 2.94$ where $f(r_1) \approx -1.10$. The convergence of $r^2 f$ for large r is rapid; in fact, it is easily shown that

$$r^2 f - C \sim \tfrac{1}{4} r^4 \, \mathrm{e}^{-r^2/4} \quad \text{as} \quad r \to \infty. \tag{2.31}$$

Assuming for the moment that $g(r) = 0$, we now have ψ to order ϵ in the form

$$\psi = \psi_0(r) + \epsilon_1 f(r) \sin 2\theta, \tag{2.32}$$

where $\epsilon_1 = \epsilon\lambda$. The corresponding vorticity is

$$\omega = \omega_0(r) + \epsilon_1 \Omega(r) \sin 2\theta, \tag{2.33}$$

where

$$\Omega(r) = -r^{-1}(rf')' + 4r^{-2} f = (\tfrac{1}{4} r^2 - f)\,\eta \tag{2.34}$$

using (2.25). Clearly $\Omega(r) \leqslant 0$ for all r (figure 3). Note the asymptotic behaviour

$$\Omega(r) \sim -\tfrac{1}{4}(1-4a)(r^2 - \tfrac{5}{24} r^4 + \ldots) \quad \text{for} \quad r \ll 1, \tag{2.35}$$

and

$$\Omega(r) \sim -\tfrac{1}{16} r^4 \, \mathrm{e}^{-r^4/4} \quad \text{as} \quad r \to \infty. \tag{2.36}$$

We note a potential difficulty here, in that

$$\frac{\Omega(r)}{\omega_0(r)} \sim -\frac{\pi}{4} r^4 \quad \text{as} \quad r \to \infty, \tag{2.37}$$

so that the 'leading' term $\omega_0(r)$ in (2.33) is not dominant for large r. However, it *is* dominant provided

$$r^2 \ll 2(\pi\epsilon_1)^{-\frac{1}{2}}, \tag{2.38}$$

and when $r^2 \sim 2(\pi\epsilon_1)^{-\frac{1}{2}}$, both $\omega_0(r)$ and $\epsilon_1 \Omega(r)$ are of order $(4\pi)^{-1} \exp[-\frac{1}{2}(\pi\epsilon_1)^{-\frac{1}{2}}]$, i.e. transcendentally small. We discuss this point further in §5.

The streamlines are now given, to order ϵ_1, by

$$r = r_0 + \epsilon_1 r_\psi(\theta), \tag{2.39}$$

where, by substituting in (2.32) and equating terms of order ϵ_1,

$$r_\psi(\theta) = -\frac{f(r_0)}{\psi_0'(r_0)} \sin 2\theta = \frac{f(r_0)}{v_0(r_0)} \sin 2\theta. \tag{2.40}$$

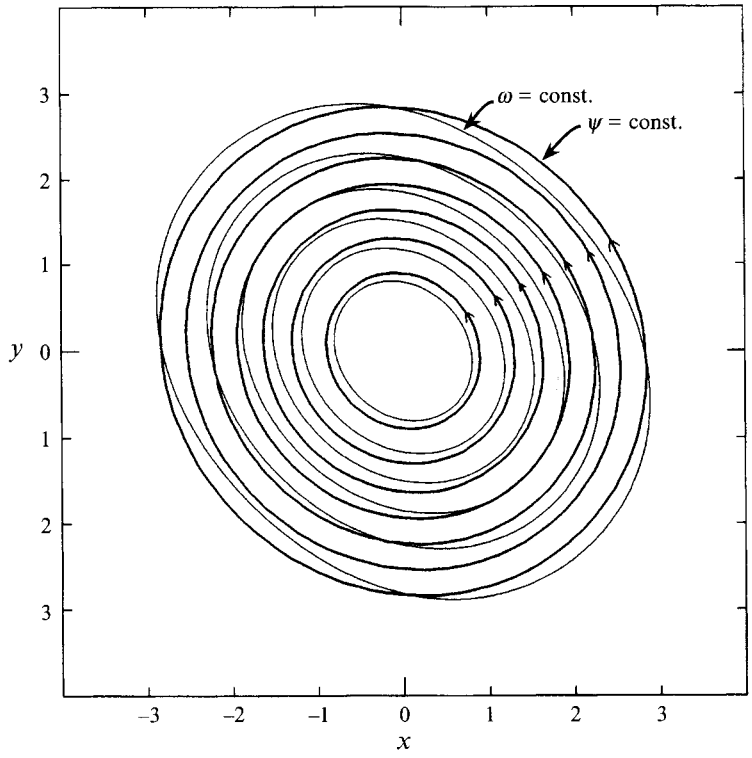

FIGURE 4. Contours ψ = const. (thick) and ω = const. (thin) obtained from (2.32) and (2.33) with $\epsilon_1 = 0.005$. Note that the streamlines are quite nearly circular, whereas the iso-vorticity lines are more strongly flattened. (Contour levels: $\psi = -0.015n$ $(n = 1, 2, \ldots, 7)$; $\omega = \omega_{min} + (\omega_{max} - \omega_{min})n/7$ $(n = 1, 2, \ldots, 6)$; $\omega_{min} = -4.737 \times 10^{-4}$, $\omega_{max} = 7.938 \times 10^{-2}$.)

Thus, the streamlines are ellipses with major axes on $\theta = 3\pi/4, 7\pi/4$ and minor axes on $\theta = \pi/4, 5\pi/4$ (because $f(r_0)/v_0(r_0) < 0$); the eccentricity of these ellipses is maximal at $r_0 \approx 3.9$.

Similarly provided $\epsilon_1 \ll 1$ and $r^2 \ll 2(\pi\epsilon_1)^{-\frac{1}{2}}$, the lines of constant vorticity are given by

$$r = r_0 + \epsilon_1 r_\omega(\theta), \tag{2.41}$$

where

$$r_\omega(\theta) = -\frac{\Omega(r_0)}{\omega_0'(r_0)} \sin 2\theta = -2\pi r_0 \left[\frac{\frac{1}{4}r_0^2 - f(r_0)}{1 - e^{-r_0^2/4}}\right] \sin 2\theta. \tag{2.42}$$

Again, these are ellipses with the same orientation of major and minor axes as above, a property that is evident in the iso-vorticity plots of KO92 (figure 13*d–f*) for $R_\Gamma \gtrsim 100$. The tendency of the principal axes of the iso-vorticity ellipses to rotate in a counterclockwise sense from the principal axes of strain $(x = 0, y = 0)$ was noted by Robinson & Saffman (1984); the present analysis shows that the total angle of rotation asymptotes to $\frac{1}{4}\pi$ as $R_\Gamma \to \infty$.

Although the principal axes of streamline ellipses and iso-vorticity ellipses coincide, the curves do not themselves coincide because the eccentricities at given r_0 are clearly different in the two cases. At order ϵ, vorticity is no longer constant on streamlines; the slight mismatch is accommodated by the strain field and by viscous diffusion. The situation is illustrated for the case $\epsilon_1 = 0.005$ in figure 4, which shows contours of ψ and ω based on (2.32) and (2.33). Note that, despite the quite strong ellipticity of the

iso-vorticity lines, the streamlines settle down rapidly to circular form outside the vortex core.

Proof that $g(r) \equiv 0$

Consider now the terms of order ϵ^2 in (2.7); these give

$$-\frac{1}{r}\left[\frac{\partial(\psi_2,\omega_0)}{\partial(r,\theta)}+\frac{\partial(\psi_0,\omega_2)}{\partial(r,\theta)}\right]=\frac{1}{r}\frac{\partial}{\partial\theta}(\omega_0'\psi_2+v_0\omega_2)=\mathrm{L}_0\omega_1+\lambda\mathrm{L}_1\omega_1+\frac{1}{r}\frac{\partial(\psi_1,\omega_1)}{\partial(r,\theta)}. \quad (2.43)$$

All the terms in $\lambda\mathrm{L}_1\omega_1$ and $r^{-1}\partial(\psi_1,\omega_1)/\partial(r,\theta)$ are proportional to $\sin 2\theta$ or $\cos 2\theta$ (for details see §4 below), and so give zero when integrated from $\theta = 0$ to $\theta = 2\pi$. Hence, integrating (2.43) over θ gives the solvability condition

$$\mathrm{L}_0(-\nabla^2 g) = 0 \quad (2.44)$$

using the vorticity $\omega_1 = -\nabla^2\psi_1$ with ψ_1 given by (2.24). It follows that

$$\nabla^2 g = k\,\mathrm{e}^{-r^2/4} \quad (2.45)$$

for some constant k. The normalization condition coupled with the zero-order solution (2.19) now implies that $k = 0$. Hence $\nabla^2 g(r) = 0$ and the only solution finite at $r = 0$ is $g = \text{const.}$; since an additive constant in the streamfunction does not affect the flow, we may clearly take $g \equiv 0$, as anticipated above.

3. Spatial distribution of viscous dissipation

Let s_{ij} be the (dimensionless) rate-of-strain tensor, with elements

$$\{s_{ij}\}=\begin{pmatrix}\alpha+\partial u_x/\partial x & \frac{1}{2}(\partial u_x/\partial y+\partial u_y/\partial x) & 0\\ \frac{1}{2}(\partial u_x/\partial y+\partial u_y/\partial x) & \beta+\partial u_y/\partial y & 0\\ 0 & 0 & 1\end{pmatrix}. \quad (3.1)$$

Then the rate of viscous dissipation is given by

$$\Phi = 2s_{ij}s_{ij} = 2[D+\epsilon^2(\tfrac{1}{2}\lambda^2+\tfrac{3}{2})], \quad (3.2)$$

where

$$D = 2\psi_{xy}^2+\tfrac{1}{2}(\psi_{xx}-\psi_{yy})^2-2\epsilon_1\psi_{xy}, \quad (3.3)$$

and, as before, $\epsilon_1 = \lambda\epsilon$. (The *dimensional* dissipation rate is given by $\nu(\Gamma/\delta)^2\Phi = (\gamma^2\Gamma^2/\nu)\,\Phi$.) The term $\epsilon^2(\frac{1}{2}\lambda^2+\frac{3}{2})$ in (3.2) comes from the background strain field and is the uniform value of $\frac{1}{2}\Phi$ far from the vortex; hence D represents the excess of $\frac{1}{2}\Phi$ over this background values due to the presence of the vortex. Converting to polar coordinates, (3.3) becomes

$$\begin{aligned}D(r,\theta) = {}&\tfrac{1}{2}(\psi_{rr}-r^{-1}\psi_r-r^{-2}\psi_{\theta\theta})^2+2r^{-2}(\psi_{r\theta}-r^{-1}\psi_\theta)^2\\ &-\epsilon_1(\psi_{rr}-r^{-1}\psi_r-r^{-2}\psi_{\theta\theta})\sin 2\theta-2\epsilon_1 r^{-1}(\psi_{r\theta}-r^{-1}\psi_\theta)\cos 2\theta. \quad (3.4)\end{aligned}$$

It proves necessary to consider terms up to order ϵ^2 in this expression, in order to get a uniformly valid first approximation to D. Substituting $\psi = \psi_0(r)+\epsilon_1 f(r)\sin 2\theta+\epsilon^2\psi_2(r,\theta)$, we obtain

$$\begin{aligned}D(r,\theta) = {}&\tfrac{1}{2}(H(r))^2-\epsilon_1 H(r)(1-G(r))\sin 2\theta+\epsilon_1^2[(\tfrac{1}{2}G^2-G)\sin^2 2\theta+(\tfrac{1}{2}F^2-F)\cos^2 2\theta]\\ &+\epsilon^2 H(r)\,G_2(r,\theta)+O(\epsilon^3), \quad (3.5)\end{aligned}$$

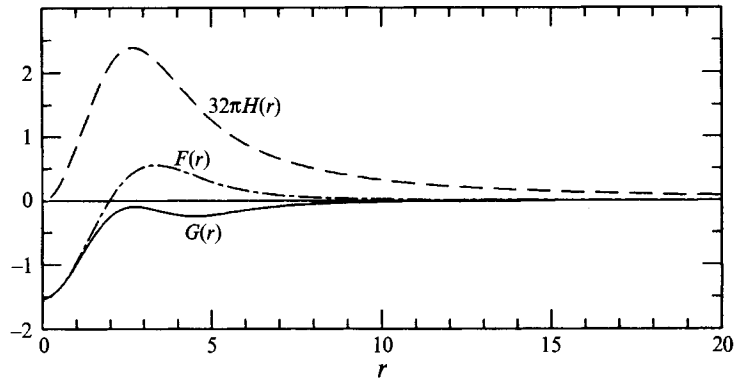

FIGURE 5. The functions $F(r)$ (chain-dashed), $G(r)$ (solid), $32\pi H(r)$ (dashed) given by (3.6), (3.7) and (3.8).

where
$$F(r) = 4r^{-1}(f' - r^{-1}f), \tag{3.6}$$
$$G(r) = f'' - r^{-1}f' + 4r^{-2}f, \tag{3.7}$$
$$H(r) = \psi_0'' - r^{-1}\psi_0' = -r\left(\frac{v_0}{r}\right)' = \frac{1}{\pi r^2} - \left(\frac{1}{4\pi} + \frac{1}{\pi r^2}\right)e^{-r^2/4}, \tag{3.8}$$
and
$$G_2(r,\theta) = \psi_{2rr} - r^{-1}\psi_{2r} - r^{-2}\psi_{2\theta\theta}. \tag{3.9}$$
The functions F, G, H are shown in figure 5. Note the following asymptotic behaviour: for small r,
$$F(r) \sim 4a + (\tfrac{1}{4} - a)r^2 - \tfrac{25}{192}(\tfrac{1}{4} - a)r^4 + \ldots, \tag{3.10a}$$
$$G(r) \sim 4a + (\tfrac{1}{4} - a)r^2 - \tfrac{35}{192}(\tfrac{1}{4} - a)r^4 + \ldots, \tag{3.10b}$$
$$H(r) \sim \frac{1}{32\pi}(r^2 - \tfrac{1}{6}r^4 + \ldots); \tag{3.10c}$$
and as $r \to \infty$,
$$F(r) \sim -\frac{12C}{r^4} + O(r^2\, e^{-r^2/4}), \tag{3.11a}$$
$$G(r) \sim \frac{12C}{r^4} + O(r^4\, e^{-r^2/4}), \tag{3.11b}$$
$$H(r) \sim \frac{1}{\pi r^2} + O(e^{-r^2/4}). \tag{3.11c}$$
The presence of the small factor $(32\pi)^{-1} \approx 0.01$ in (3.10c) is rather striking; looking at the structure of (3.5) suggests that, for numerical purpose, $32\pi\epsilon_1$ might be a more appropriate expansion parameter than ϵ_1 (see the asymptotic behaviour of $D(r,\theta)$ as $r \to 0$, obtained below (3.15)). Note also that
$$H'(r) = 0 \quad \text{and} \quad H(r) = H_{max} \approx 0.0237 \quad \text{at} \quad r = r_c \approx 2.67, \tag{3.12}$$
and that $G(r) < 0$ for all r. Note finally that the functions $F(r)$ and $G(r)$ are almost identical for $r \lesssim 1$, where the first two terms of (3.10a, b) give an excellent approximation to both functions.

The function $\psi_2(r,\theta)$ is determined in §4. All we need note here is that

as $r \to 0$,
$$\psi_2 = O(r^2) \quad \text{and so} \quad G_2 = O(1), \tag{3.13a}$$
and as $r \to \infty$,
$$\psi_2 = O(r^{-2}) \quad \text{and so} \quad G_2 = O(r^{-4}). \tag{3.13b}$$

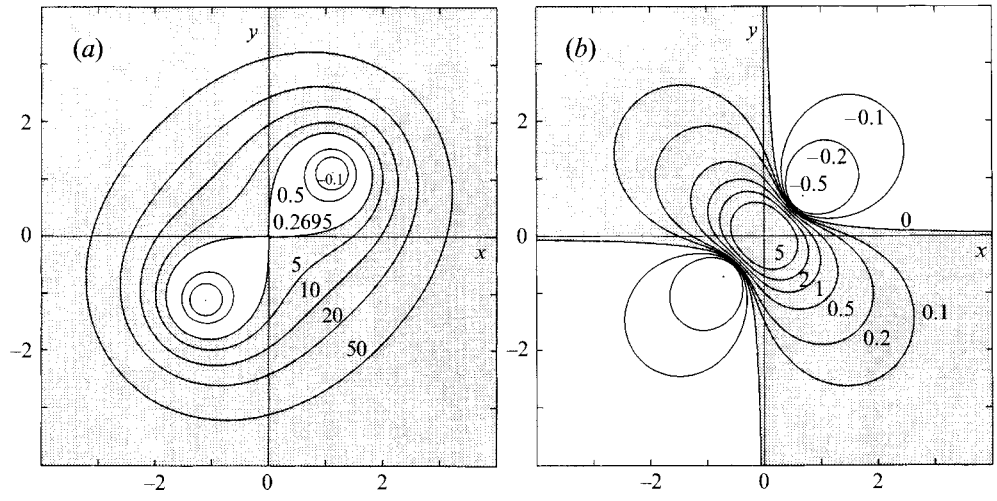

FIGURE 6. Contour plots (*a*) of the inner dissipation function $\epsilon_1^{-2}\hat{D}(\hat{r},\theta)$ defined by (3.15) and (*b*) of the outer dissipation function $\epsilon_1^{-2}\tilde{D}(\tilde{r},\theta)$ defined by (3.19).

The structure of the dissipation field (3.5) may be best understood by considering three regions.

(i) $r = O(\epsilon_1^{\frac{1}{2}})$

Defining an 'inner variable'

$$\hat{r} = (32\pi\epsilon_1)^{-\frac{1}{2}} r, \tag{3.14}$$

the leading-order contribution to D in the region where $\hat{r} = O(1)$ is

$$\hat{D}(\hat{r},\theta) \sim \epsilon_1^2[\tfrac{1}{2}\hat{r}^4 - (1-4a)\hat{r}^2 \sin 2\theta + 4a(2a-1)], \tag{3.15}$$

the final term coming from the third term of (3.5). The need to retain terms of order ϵ^2 in (3.5) should now be clear; note however that the final term of (3.5) makes no contribution to (3.15) since

$$\epsilon^2 H(r)\, G_2(r,\theta) = O(\epsilon^2 r^2) = O(\epsilon^4 \hat{r}^2) \tag{3.16}$$

in this region. The function $\epsilon_1^{-2}\hat{D}(\hat{r},\theta)$ defined by (3.15) has universal form independent of both λ and $\epsilon = 1/R_\Gamma$; its contours are shown in figure 6(*a*). It is minimal at $\hat{r} = (1-4a)^{\frac{1}{2}} \approx 1.59$, $\theta = \pi/4,\ 5\pi/4$, and there

$$\hat{D}_{min} = -0.5\epsilon_1^2. \tag{3.17}$$

(ii) $r = O(\epsilon_1^{-\frac{1}{2}})$

Similarly, defining an 'outer variable'

$$\tilde{r} = (\pi\epsilon_1)^{\frac{1}{2}} r, \tag{3.18}$$

we find that in the region where $\tilde{r} = O(1)$, the leading contribution to (3.5) is

$$\tilde{D}(\tilde{r},\theta) \sim \epsilon_1^2[\tfrac{1}{2}\tilde{r}^{-4} - \tilde{r}^{-2}\sin 2\theta]. \tag{3.19}$$

Again, $\epsilon_1^{-2}\tilde{D}(r,\theta)$ has universal form; its contours are shown in figure 6(*b*). It is minimal at $\tilde{r} = 1$, $\theta = \pi/4,\ 5\pi/4$, and there we again find

$$\tilde{D}_{min} = -0.5\epsilon_1^2. \tag{3.20}$$

(Actually, as noted below (2.37), the asymptotic solution is suspect for $r \gtrsim \epsilon_1^{-\frac{1}{4}}$, and is certainly invalid in the outermost region $r \gg \epsilon_1^{-\frac{1}{2}}$; this is discussed further in §5 and in Appendix A.) The results (3.17) and (3.20) imply that the corresponding minima of Φ are given by

$$\tfrac{1}{2}\Phi_{min} = \tfrac{3}{2}\epsilon^2, \tag{3.21}$$

independent of λ.

(iii) $r = O(1)$

When $r = O(1)$, it is sufficient to retain the first two terms of (3.5), i.e.

$$D(r,\theta) \sim D_1(r,\theta) = \tfrac{1}{2}(H(r))^2 - \epsilon_1 H(r)(1-G(r))\sin 2\theta. \tag{3.22}$$

This function is symmetric about the diagonal lines $x = \pm y$, and since $H(r)(1-G(r)) > 0$ for all $r > 0$, D is maximal as a function of θ on $x = -y$, minimal on $x = y$. In the limit $\epsilon_1 = 0$, the contours $D_1(r,\theta) = \text{const.}$ become circles $r = \text{const.}$ (a behaviour that may be seen both in the outer limit $\hat{r} \to \infty$ of (3.15) and in the inner limit $\tilde{r} \to 0$ of (3.19)) and D_1 is maximal where $H(r)$ is maximal, i.e. at $r = r_c \approx 2.67$. This maximum value is thus, asymptotically,

$$D_{1max} \sim \tfrac{1}{2}H_{max}^2 \approx 2.808 \times 10^{-4}. \tag{3.23}$$

The perturbation term in (3.22) breaks this circular symmetry, and, provided we avoid the critical circle $r = r_c$, the contours are given to first order in ϵ_1 by

$$r = r_0 + \epsilon_1 r_D(\theta), \tag{3.24}$$

where, by substituting in (3.22) and linearizing,

$$r_D(\theta) = \frac{1-G(r_0)}{H'(r_0)}\sin 2\theta. \tag{3.25}$$

These contours are ellipses, with major axis $x = -y$ for $H'(r_0) < 0$, i.e. $r_0 > r_c$, and with major axis $x = y$ for $H'(r_0) > 0$, i.e. $r_0 < r_c$.

This approximation is clearly invalid near $r_0 = r_c$ where $H'(r_0) = 0$. Near this value,

$$H(r) \approx H_c + \tfrac{1}{2}(r-r_c)^2 H_c'', \tag{3.26}$$

where $H_c = H(r_c), H_c'' = H''(r_c)$, so that (3.22) becomes

$$D_1(r,\theta) \approx \tfrac{1}{2}H_c^2 + \tfrac{1}{2}(r-r_c)^2 H_c H_c'' - \epsilon_1 H_c(1-G_c)\sin 2\theta, \tag{3.27}$$

and the contour

$$D = \tfrac{1}{2}H_c^2 - \epsilon_1 H_c(1-G_c) = (0.028 - 2.6\epsilon_1)\times 10^{-2} = D_s, \tag{3.28}$$

say, is given by

$$(r-r_c)^2 = 2\epsilon_1 \frac{1-G_c}{|H_c''|}(1-\sin 2\theta). \tag{3.29}$$

This is a separatrix joining saddle points at $r = r_c$, $\theta = \pi/4, 5\pi/4$. Maxima of D occur at $r = r_c$, $\theta = 3\pi/4, 7\pi/4$, and there

$$D_{max} = \tfrac{1}{2}H_c^2 + \epsilon_1 H_c(1-G_c) = (0.028 + 2.6\epsilon_1)\times 10^{-2}. \tag{3.30}$$

There is a 'cat's eye' structure with width (at $\theta = 3\pi/4, 7\pi/4$) given from (3.29) by

$$\Delta r = \frac{4(1-G_c)^{\frac{1}{2}}}{|H_c''|^{\frac{1}{2}}}\epsilon_1^{\frac{1}{2}} \approx 13.2\epsilon_1^{\frac{1}{2}}. \tag{3.31}$$

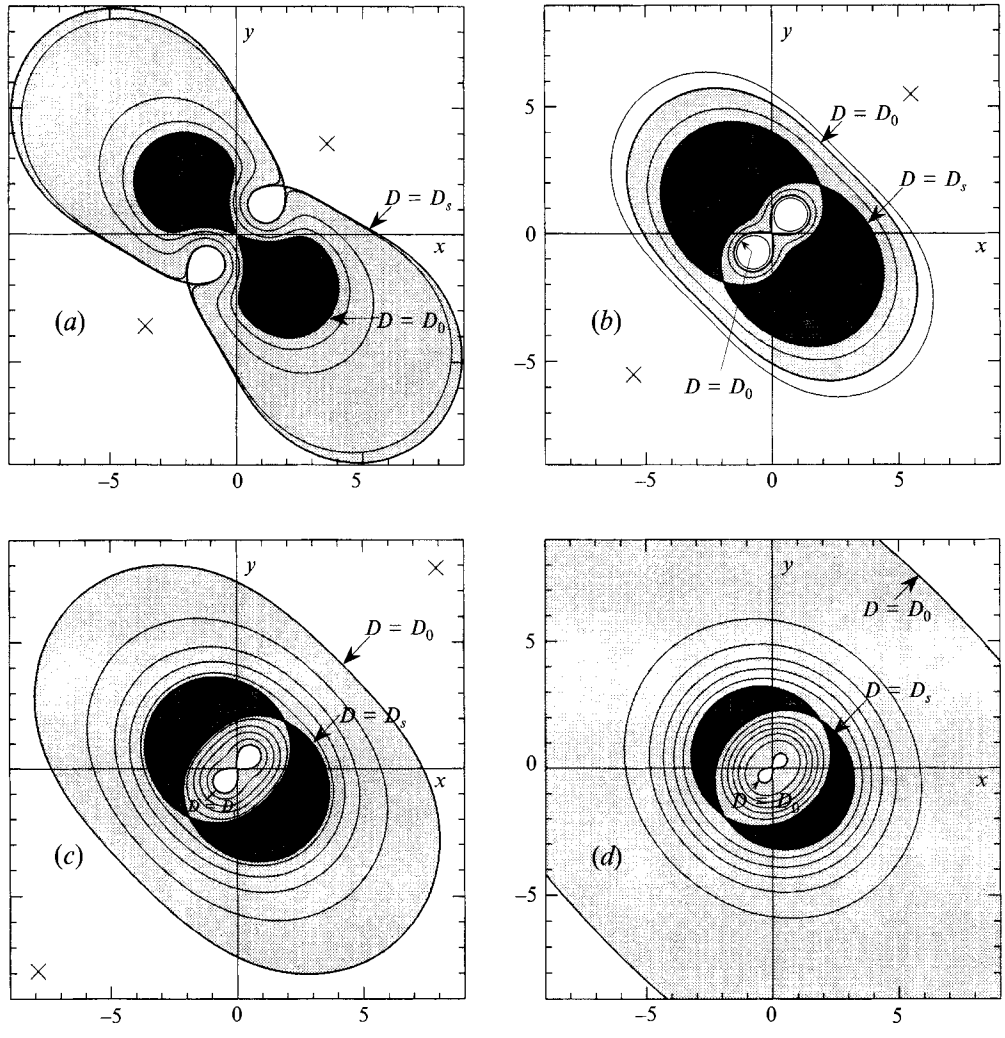

FIGURE 7. Contour plots of the dissipation function $D(r,\theta)$ defined by (3.32). The maxima of D are marked with * and the (global) minima with $\times$. The contour levels are equally spaced at one-seventh of the difference $D_{max}-D_{min}$. The separatrices $D=D_0$ and $D=D_s$ are also included (thick lines), and the plots are shaded light grey where $\min(D_0,D_s)<D<\max(D_0,D_s)$ and dark grey where $D>\max(D_0,D_s)$. (*a*) $\epsilon_1=\lambda/R_\Gamma=0.01$ $(D_0>D_s)$, (*b*) $\epsilon_1=0.005$ $(D_s>D_0)$, (*c*) $\epsilon_1=0.0025$ $(D_s>D_0)$, (*d*) $\epsilon_1=0.001$ $(D_s>D_0)$. Compare with the computed contours in figure 14(*c–f*) of KO92.

All of these features may be observed in figure 7(*d*) which shows contours of the function (3.32) below for $\epsilon_1=0.001$.

The above discussion makes it clear that a uniformly valid approximation to $D(r,\theta)$ for small ϵ is given by simply omitting the term $\epsilon^2 H(r)\,G_2(r,\theta)$ in (3.5) which is always dominated by other terms. Thus

$$D(r,\theta)\sim \tfrac{1}{2}(H(r))^2-\epsilon_1 H(r)(1-G(r))\sin 2\theta + \epsilon_1^2[(\tfrac{1}{2}G^2-G)\sin^2 2\theta+(\tfrac{1}{2}F^2-F)\cos^2 2\theta]. \quad (3.32)$$

Contours of this function are shown in figure 7 for $\epsilon_1=0.01$, 0.005, 0.0025, 0.001. These values are chosen to enable comparison with the contours obtained numerically

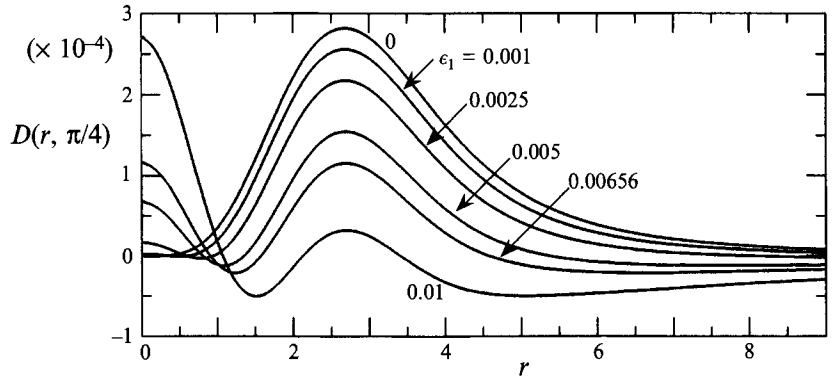

FIGURE 8. The function $D(r,\pi/4)$ defined by (3.34) for various values of ϵ_1. A saddle point of $D(r,\theta)$ occurs very near the point where $D(r,\pi/4)$ is maximal. When $\epsilon_1 \approx 0.00656$, the value D_s at this saddle equals $D_0 \approx 2.69\epsilon_1^2$.

and presented in figure 14(*c–f*) of KO92. The value $\epsilon_1 = 0.01$ (for which $32\pi\epsilon_1 \approx 1$) is the largest for which the present asymptotic theory can reasonably be applied. The separatrices

$$D = D_0 = 4a(2a-1)\epsilon_1^2 \approx 2.69\epsilon_1^2 \tag{3.33}$$

through the origin and $D = D_s$ through the other saddle points on $x = y$, are included in each case, and the contour plots are shaded light grey in the region where $\min(D_0, D_s) < D < \max(D_0, D_s)$, and dark grey where $D > \max(D_0, D_s)$. The following points should be noted: (i) the inner region ($\hat{r} = O(1)$) is best seen in figure 7(*d*) ($\epsilon_1 = 0.001$) (compare with figure 6*a*) and the outer region is best seen in figure 7(*a*) ($\epsilon_1 = 0.01$) (compare with figure 6*b*); (ii) the cat's eye pattern and the ellipses both inside and outside are best seen in figure 7(*d*); (iii) in all cases, the regions (dark grey) of strong dissipation are set distinctly off-centre on the diagonal $x = -y$, very much as revealed in the corresponding computations of KO92.

There is a change of topology of these contours as ϵ_1 increases from very small levels. This may be understood from consideration of the function

$$D(r,\pi/4) = \tfrac{1}{2}(H(r))^2 - \epsilon_1 H(r)(1-G(r)) + \epsilon_1^2(\tfrac{1}{2}G^2 - G) \tag{3.34}$$

shown in figure 8 for various values of ϵ_1. The change of topology occurs when $\epsilon_1 = \epsilon_{1c} \approx 0.00656$, at which value $D_0 = D_s$. The corresponding contour plot is shown in figure 9. There are further interesting changes in the topology of $D(r,\theta)$ for larger values of ϵ_1, but these lie beyond the range of validity of the asymptotic analysis, and are therefore not considered here.

The most striking property of the field of dissipation (3.32) is that, as $\epsilon_1 \to 0$, the dissipation becomes quite sharply concentrated near the radius $r = 2.67$ at which $H(r)$ is maximal. At this radius,

$$\frac{\omega_0(r)}{\omega_0(0)} = \mathrm{e}^{-r^2/4} = 0.166,$$

so that the enstrophy $(\omega_0(r))^2$ is only $0.028(\omega(0))^2$, i.e. 2.8 % of its maximum value. This means that the region of large enstrophy and large dissipation are effectively non-overlapping, an important conclusion in the turbulence context (see §6 below). The θ-averaged enstrophy and dissipation, correct to order ϵ, are given by

$$\langle\omega^2\rangle = (\omega_0(r))^2 = (16\pi^2)^{-1}\,\mathrm{e}^{-r^2/2}, \quad 2\langle D\rangle = (H(r))^2, \tag{3.35}$$

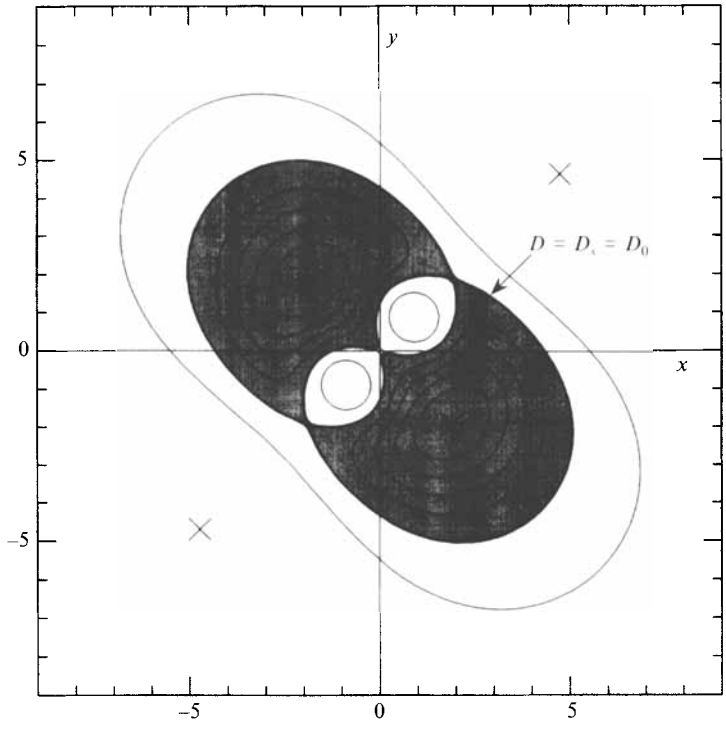

FIGURE 9. Contour plot of $D(r,\theta)$ for the critical case $\epsilon_1 = \epsilon_{1c} \approx 0.00656$ ($D_0 = D_s$). Shaded area as in figure 7.

and it is not hard to verify that

$$\int_0^\infty (H(r))^2 r\,\mathrm{d}r = \int_0^\infty (\omega_0(r))^2 r\,\mathrm{d}r = (16\pi^2)^{-1}. \tag{3.36}$$

It is also easy to verify that at $r = \sqrt{2}$,

$$\frac{(H(r))^2}{H_{max}^2} = \frac{(\omega_0(r))^2}{\omega_{max}^2} = \mathrm{e}^{-1} = 0.368 \tag{3.37}$$

and that

$$\int_0^{\sqrt{2}} (\omega_0(r))^2 r\,\mathrm{d}r = 0.632 \int_0^\infty (\omega_0(r))^2 r\,\mathrm{d}r, \tag{3.38}$$

and

$$\int_0^{\sqrt{2}} (H(r))^2 r\,\mathrm{d}r = 0.0128 \int_0^\infty (H(r))^2 r\,\mathrm{d}r. \tag{3.39}$$

Hence 63.2% of the total enstrophy associated with the vortex lies within the radius $r = \sqrt{2}$, whereas 98.7% of the viscous dissipation occurs outside this radius.

The correlation between the fields $\omega_0(r)$ and $H(r)$ is given by

$$\rho_1 = \frac{\int_0^\infty \omega_0(r)\,H(r)\,r\,\mathrm{d}r}{\left(\int_0^\infty \omega_0^2 r\,\mathrm{d}r \int_0^\infty H^2 r\,\mathrm{d}r\right)^{\frac{1}{2}}} = \frac{1}{16\pi^2}\int_0^\infty \omega_0(r)\,H(r)\,r\,\mathrm{d}r. \tag{3.40}$$

This integral can be evaluated, with the result

$$\rho_1 = -1 + 2\ln 2 = 0.386. \tag{3.41}$$

	$(2\epsilon^2)^{-1}\Phi_{max}$			$(2\epsilon^2)^{-1}\Phi_{min}$	
ϵ_1	From (3.32)	From (3.30)	Numerical	From (3.32)	Numerical
(*a*) 0.01	3.00	2.98	2.90	1.50	1.50
(*b*) 0.005	5.76	5.73	5.57	1.50	1.50
(*c*) 0.0025	15.5	15.4	15.1	1.50	1.50
(*d*) 0.001	79.1	78.1	77.3	1.50	1.50

TABLE 1. Maximum and minimum dissipation rate for the case $\lambda = \frac{1}{2}$. The numerical values were obtained by integrating (A 3) by the finite difference method as in KO92 with a larger domain ($-15 \leqslant x, y \leqslant 15$) and a finer mesh ($\Delta x = \Delta y = 0.25$).

The correlation between the enstrophy field $(\omega(r,\theta))^2$ and the dissipation field $D(r,\theta)$ is given, correct to order ϵ, by

$$\rho_2 = \frac{\int_0^\infty \omega_0^2 H^2 r\,\mathrm{d}r}{\left(\int_0^\infty \omega_0^4 r\,\mathrm{d}r \int_0^\infty H^4 r\,\mathrm{d}r\right)^{\frac{1}{2}}} + O(\epsilon^2). \tag{3.42}$$

The integrals have been evaluated numerically, with the result

$$\begin{aligned}\rho_2 &= \frac{1.157\times10^{-6}}{[(2.005\times10^{-5})\times(1.882\times10^{-6})]^{\frac{1}{2}}} + O(\epsilon^2)\\ &= 0.19 + O(\epsilon^2).\end{aligned} \tag{3.43}$$

The results (3.41), (3.43) should be testable through appropriate manipulation of DNS data.†

Finally, we note some numerical comparisons. Table 1 shows the maximum and minimum values of $\Phi/2\epsilon^2$ obtained from the function (3.32) for the case $\lambda = \frac{1}{2}$, together with the corresponding figures computed for this case by KO92. The minimum values are in perfect agreement. There is however a systematic difference of about 10% between the maxima given by the asymptotic theory and the maxima previously computed. The reason for this difference is that, for the larger values of ϵ_1, the asymptotic theory is perhaps not sufficiently accurate, while for the smaller values of ϵ_1, the numerical procedure of KO92 is slow to converge. We have repeated the computation of KO92 for the case $\lambda = \frac{1}{2}$, $R_\Gamma = 500$ (i.e. $\epsilon_1 = 0.001$) using a larger domain and a finer mesh, and the discrepancy between the numerical solution and the asymptotic theory is indeed reduced (see Table 1).

4. Higher-order asymptotics

Let us now briefly consider the problem posed by (2.43) at order ϵ^2. As shown at the end of §2, the solvability condition for this equation yields the result $g(r) = 0$. Then, (2.43) simplifies to the form

$$\frac{\partial}{\partial\theta}(\omega_0'\psi_2 + v_0\omega_2) = 2\lambda v_0(r)\,M(r)\sin 2\theta + 4\lambda^2 v_0(r)\,N(r)\sin 4\theta, \tag{4.1}$$

† As pointed out by a referee, ρ_2 is zero for a Rankine vortex (for which the enstrophy is non-zero only for $r < \delta$ and the dissipation is non-zero only for $r > \delta$). On the other hand, $\rho_2 = 1$ for a vortex layer in which $\boldsymbol{\omega} = (0, 0, \omega(y))$ and dissipation is proportional to enstrophy (Tanaka & Kida 1993).

where
$$M(r) = \frac{r}{2v_0(r)}(\Omega'' + (\tfrac{1}{2}r + r^{-1})\Omega' + (1-4r^{-2})\Omega), \tag{4.2}$$

$$N(r) = \frac{1}{16v_0(r)}(r^2\Omega' - 2r\Omega - 4(f\Omega' - f'\Omega)). \tag{4.3}$$

Integrating (4.1) with respect to θ and dividing by $v_0(r)$, we obtain

$$\nabla^2\psi_2 - \eta(r)\psi_2 = \lambda M(r)\cos 2\theta + \lambda^2 N(r)\cos 4\theta + g_2(r), \tag{4.4}$$

for some function $g_2(r)$.

The solution of (4.4) may be sought in the form

$$\psi_2(r,\theta) = \lambda^2\psi_{02}(r) + \lambda f_2(r)\cos 2\theta + \lambda^2 f_4(r)\cos 4\theta, \tag{4.5}$$

where
$$\mathrm{L}_2 f_2 \equiv f_2'' + r^{-1}f_2' - 4r^{-2}f_2 = \eta f_2 + M(r), \tag{4.6}$$

and
$$\mathrm{L}_4 f_4 \equiv f_4'' + r^{-1}f_4' - 16r^{-2}f_4 = \eta f_4 + N(r). \tag{4.7}$$

The function ψ_{02} is determined by a solvability condition at $O(\epsilon^3)$ (see Appendix B). Note that the equation $\mathrm{L}_2 f = 0$ has linearly independent solutions r^2 and r^{-2}, while the equation $\mathrm{L}_4 f = 0$ has linearly independent solutions r^4 and r^{-4}.

Now, using (2.28) and (2.35), the behaviour of M and N for small r may be calculated, and is

$$M(r) \sim \tfrac{1}{2}\pi(1-4a)r^2, \quad N(r) \sim -\tfrac{1}{32}\pi(1-4a)^2 r^4. \tag{4.8}$$

Similarly, from (2.31) and (2.36), we find that

$$M(r) \sim -\tfrac{1}{64}\pi r^8 \,\mathrm{e}^{-r^2/4}, \quad N(r) \sim -\tfrac{1}{256}\pi r^8 \,\mathrm{e}^{-r^2/4} \quad \text{as} \quad r \to \infty. \tag{4.9}$$

These properties guarantee that solutions of (4.6) and (4.7) may be found with the properties

$$f_2 \sim a_2 r^2 \quad \text{as} \quad r \to 0, \qquad f_2 \sim C_2 r^{-2} \quad \text{as} \quad r \to \infty, \tag{4.10}$$

$$f_4 \sim a_4 r^4 \quad \text{as} \quad r \to 0, \qquad f_4 \sim C_4 r^{-4} \quad \text{as} \quad r \to \infty. \tag{4.11}$$

Hence the solution (4.5) is uniquely determined. Again it has the property that the associated vorticity $\omega_2 = -\nabla^2\psi_2$ is exponentially small as $r \to \infty$.

The streamfunction $\psi = \psi_0 + \epsilon\psi_1 + \epsilon^2\psi_2$ now has the form

$$\psi = \psi_0(r) + \epsilon\lambda f(r)\sin 2\theta + \epsilon^2(\lambda^2\psi_{02}(r) + \lambda f_2(r)\cos 2\theta + \lambda^2 f_4(r)\cos 4\theta) + O(\epsilon^3). \tag{4.12}$$

Note that ψ now involves ϵ and λ independently, and not just through the combination $\epsilon_1 = \epsilon\lambda$. Moreover, the symmetry about the diagonals $x = \pm y$ is clearly broken at order ϵ^2, and this will carry over to the dissipation function also.

This procedure may now be carried to higher orders in ϵ if required. The main point to note here is that a well-defined procedure exists. This lends confidence to our claim that the essential features of the flow are well captured by the first two terms of the expansion (2.11) when ϵ is sufficiently small.

5. The case $\lambda > 1$ (biaxial strain)

The asymptotic solution that we have obtained in §2 appears to be valid whether $\lambda < 1$, or $\lambda > 1$, provided merely that $\epsilon_1 = \epsilon\lambda \ll 1$. This suggest that concentrated vortices should be able to survive even in a biaxial strain field where both β and γ are positive.

There are two difficulties here, the first of which we have already noted in relation to the behaviour (2.37) of the ratio $\Omega(r)/\omega_0(r)$ for large r. The fact that $\epsilon_1|\Omega(r)|$ eventually becomes of the same order of magnitude as $\omega_0(r)$ means that the expansion (2.11) cannot be uniformly valid all the way to $r = \infty$. However, at the large values of r (of order $\epsilon_1^{-\frac{1}{4}}$) at which it breaks down, the vorticity is already of order $\exp[-\frac{1}{2}(\pi\epsilon_1)^{-\frac{1}{2}}]$, i.e. so small that the non-uniformity is of no consequence. (The situation is a little reminiscent of the breakdown of the 'inner solution' for Stokes flow past a sphere, a breakdown that can be rectified by the use of matched inner and outer expansions.) At very great distances ($r \gg \epsilon_1^{-\frac{1}{2}}$) the solution should match to a solution of the linearized form of (2.4). We show, in Appendix A, that the unique stable steady solution of this linearized equation is the solution (1.7). Hence in the outermost regions, the principal axes of the iso-vorticity ellipses must rotate back towards the principal axes of strain (Ox, Oy).

The second difficulty arises specifically for $\lambda > 1$. Far from the vortex core, the vorticity is exponentially small; moreover the imposed strain field $(\alpha x, \beta y, \gamma z)$ dominates (at sufficient distance) over the velocity $v_0(r) \sim \Gamma/2\pi r$ associated with the vortex. In this 'far field', the vorticity behaves like a passive scalar and when $\beta > 0$, it is convected to $y = \pm\infty$ (the linearized solution (1.7) is not available when $\beta > 0$). The strain dominates over $v_0(r)$ at a (dimensional) distance

$$r \sim \epsilon^{-\frac{1}{2}}\delta \tag{5.1}$$

from the vortex, and at distances greater than this a strictly steady solution with $\beta > 0$ is apparently not possible.

However, the vorticity is transcendentally small in this region so that the rate of reduction of the circulation $\Gamma(r)$ inside a circle of radius $r \sim \epsilon^{-\frac{1}{2}}\delta$ due to this 'stripping' mechanism† is likewise transcendentally small. In order of magnitude, when $(r/\delta)^2 \sim \epsilon^{-1}$,

$$\frac{\partial}{\partial t}\Gamma(r,t) \sim -2\pi r\beta r\frac{\gamma\Gamma}{4\pi\nu}\exp\left[-\frac{r^2}{4\delta^2}\right] \sim -\tfrac{1}{2}\beta\epsilon^{-1}\Gamma\exp\left[-\frac{1}{4\epsilon}\right] = -\frac{\Gamma}{t_s}, \tag{5.2}$$

say, so that the timescale t_s of this process is

$$t_s \sim \frac{\epsilon}{\beta}\exp\left[\frac{1}{4\epsilon}\right], \tag{5.3}$$

which is effectively infinite when $\epsilon \ll 1$. Thus, although in a strict sense equation (2.4) has no solution vanishing at infinity when $\beta > 0$, the 'solution' that we have obtained in §2 is *quasi-steady* when $\beta > 0$, with a rate of loss of circulation (by stripping) that is so small as to be effectively negligible. Our conclusion is that the stretched vortex can survive for a time that is effectively infinite even when $\lambda > 1$ (i.e. $\beta > 0$).

A fortiori, the same remarks apply to the plane strain situation $\lambda = 1$ (i.e. $\beta = 0$). In this case, vorticity can be lost to $y = \pm\infty$ by viscous diffusion which (at large distances from the core) is not opposed by inward convection. The rate of loss of vorticity is likely to be even smaller than estimated above for the case $\beta > 0$, provided always that $\epsilon \ll 1$.

† The mechanism should not be confused with the *inviscid* stripping mechanism that can act on elliptical vortices in two-dimensional straining flow (Dritschel 1989, 1990; Legras & Dritschel 1993).

6. Discussion

In this paper we have obtained an asymptotic solution of the nonlinear equation describing a vortex of finite circulation Γ subject to a non-axisymmetric strain field. This solution is applicable in the limit $R_\Gamma = \Gamma/\nu \to \infty$, and is valid for all values of the parameter $\lambda = (\alpha-\beta)/(\alpha+\beta)$ representing the departure from axisymmetry in the strain field.

For $0 < \lambda < 1$, the strain field is *axial*, with $\alpha < \beta < 0$. Previous numerical evidence (Robinson & Saffman 1984; KO92) indicated the existence and structure of solutions of the governing equation (2.4) for particular values of the parameters R_Γ and λ. The great advantage of the asymptotic solution is that it is valid for arbitrary values of these parameters provided $\epsilon\lambda \ll 1$ where $\epsilon = 1/R_\Gamma$. Moreover, the solution may be analysed in detail, to explain the rather complex structure of the field of viscous dissipation revealed by the computed solution of KO92, and the manner in which this changes as R_Γ increases. The dissipation has been found to be located predominantly in the region of low enstrophy near the radius $r/\delta = 2.67$, and the correlation between dissipation and enstrophy fields has been found to be $0.19 + O(\epsilon^2)$ for $\epsilon \ll 1$.

The case $\lambda = 1$ ($\beta = 0$ or *plane* strain) is of particular interest, as noted by Neu (1984) who developed a theory of unsteady vortex development for this case, with a view to explaining vortical structures (e.g. braids) in turbulent mixing layers (Lin & Corcos 1984). The theory of the present paper is clearly applicable when $\lambda = 1$, and provides detailed steady solutions for the persistent stretched braid-type vortices that are such a characteristic feature of free-shear-layer flows.

The case $\lambda > 1$ ($\beta > 0$ or *biaxial* strain) is also of great interest. A *weak* vortex aligned with the z-axis cannot possibly survive in the presence of such a strain field: the linearized solution (1.7) is available only when both α and β are negative. However, a *strong enough* vortex may well survive because its rapid rotation always tends to re-establish the circular cross-section, thus thwarting the disruptive tendency of the positive strain rate β, although as explained in §5 an *exceedingly* slow decay of circulation is inevitable. With this reservation, the asymptotic solution that we have obtained is equally valid in the range $1 < \lambda < 3$ (corresponding to $0 > \beta < \gamma$). This may help to explain why vortices, once formed, are remarkably persistent; even if they move into an environment in which $\beta > 0$, they can continue to survive with a minor adjustment of structure, provided simply that $\epsilon_1 = \lambda/R_\Gamma$ remains very small.

Even if we move into the regime $\lambda > 3$ (i.e. $\beta > \gamma$), the asymptotic solution, with the vortex still aligned along the γ-axis of strain, apparently still exits. However, if the vortex is disturbed away from this axis of strain, it will tend to rotate towards the larger (β) axis of strain so that we revert to a situation $1 > \lambda' > 3$ with a revised ordering of (α, β, γ) and $\lambda' = (\alpha-\gamma)/(\alpha+\gamma)$. We speculate that the vortex can still persist, but rotated through $\pi/2$ from its initial direction. This argument suggests moreover that if α, β and γ vary continuously and not too rapidly with time, then the vortex must always tend to line up with an axis of positive rate of strain, this being the only stable configuration; only in exceptional circumstances therefore could it find itself aligned with an axis of negative rate of strain (which could lead to its extinction).

Thus it appears that, if and when strong vortices form through the well-understood vortex stretching mechanism, they have a good chance of surviving for a long time. A network of such *sinews* connecting and merging with regions of much weaker vorticity therefore provides an attractive starting point for the understanding of the fine-scale structure of turbulence. Further DNS investigations varying the threshold level of vorticity as well as rate of strain (see Tanaka & Kida 1993) for detection of vortex

structures is desirable to identify any competing structures that may be responsible for the balance of viscous dissipation.

This work was carried out while H. K. M. held a visiting appointment at the Research Institute for Mathematical Sciences (RIMS), Kyoto University. The kind hospitality of all at RIMS is gratefully acknowledged.

Appendix A. The far field

As noted in § 5, for $r \gg \epsilon^{-\frac{1}{2}}\delta$, the induced velocity (u_x, u_y) is negligible compared with the strain field $(\alpha x, \beta y)$, and we may therefore consider the linearized form of (2.6),

$$\alpha x \frac{\partial \omega}{\partial x} + \beta y \frac{\partial \omega}{\partial y} = \omega + \nabla^2 \omega, \tag{A 1}$$

which must hold asymptotically, irrespective of the value of ϵ $(= 1/R_\Gamma)$. We have already noted the solution

$$\omega(x, y) = \frac{(\alpha\beta)^{\frac{1}{2}}}{2\pi} \exp\left[\tfrac{1}{2}(\alpha x^2 + \beta y^2)\right] \tag{A 2}$$

when $\alpha < 0, \beta < 0$ (i.e. (1.7) in dimensionless form). We now show that this is the unique solution of (A 1) of finite circulation, and that no such solution exists if $\beta > 0$.

Consider the initial-value problem for $\omega(x, y; t)$,

$$\frac{\partial \omega}{\partial t} + \alpha x \frac{\partial \omega}{\partial x} + \beta y \frac{\partial \omega}{\partial y} = \omega + \nabla^2 \omega, \tag{A 3}$$

with

$$\omega(x, y; 0) = \omega_0(x, y), \quad \int\int \omega_0(x, y)\, \mathrm{d}x\, \mathrm{d}y = 1. \tag{A 4}$$

Equation (A 3) admits 'Kelvin mode' solutions (familiar from rapid distortion theory) of the form

$$\omega(x, y; t) = \omega(t) \exp\left[\mathrm{i}\boldsymbol{k}(t) \cdot \boldsymbol{x}\right], \tag{A 5}$$

where

$$\boldsymbol{k}(t) = (k_1(t), k_2(t)) = (k_{10}\, \mathrm{e}^{-\alpha t}, k_{20}\, \mathrm{e}^{-\beta t}), \tag{A 6}$$

and

$$\mathrm{d}\omega/\mathrm{d}t = (1 - k^2)\, \omega, \tag{A 7}$$

i.e.

$$\omega(t) = \omega_0 \exp\left[t + \frac{k_{10}^2}{2\alpha}(\mathrm{e}^{-2\alpha t} - 1) + \frac{k_{20}^2}{2\beta}(\mathrm{e}^{-2\beta t} - 1)\right]. \tag{A 8}$$

The solution of the problem (A 3), (A 4) is given by a superposition of such Kelvin modes. Let

$$\omega_0(x, y) = \int\int \hat{\omega}_0(k_{01}, k_{02})\, \mathrm{e}^{\mathrm{i}k_0 \cdot x}\, \mathrm{d}k_{01}\, \mathrm{d}k_{02}. \tag{A 9}$$

The condition of finite circulation ensures that this Fourier transform exists; and (A 4) implies that

$$\hat{\omega}_0(0, 0) = (2\pi)^{-2}. \tag{A 10}$$

Noting that

$$\frac{\partial(k_{01}, k_{02})}{\partial(k_1, k_2)} = \mathrm{e}^{(\alpha+\beta)t} = \mathrm{e}^{-t}, \tag{A 11}$$

the required solution of (A 3), (A 4) is given by

$$\omega(x,y;t) = \int\int \hat{\omega}_0(k_{01},k_{02}) \exp\left[t+\frac{k_{01}^2}{2\alpha}(\mathrm{e}^{-2\alpha t}-1)+\frac{k_{02}^2}{2\beta}(\mathrm{e}^{-2\beta t}-1)\right]\mathrm{e}^{ik\cdot x}\,\mathrm{d}k_{01}\,\mathrm{d}k_{02}$$

$$= \int\int \hat{\omega}_0(k_1\mathrm{e}^{\alpha t},k_2\mathrm{e}^{\beta t}) \exp\left[\frac{k_1^2}{2\alpha}(1-\mathrm{e}^{2\alpha t})+\frac{k_2^2}{2\beta}(1-\mathrm{e}^{2\beta t})\right]\mathrm{e}^{ik\cdot x}\,\mathrm{d}k_1\,\mathrm{d}k_2. \quad \text{(A 12)}$$

If $\alpha<0$ and $\beta<0$, then as $t\to\infty$,

$$\omega(x,y;t) \sim \int\int \hat{\omega}_0(0,0)\exp\left[\frac{k_1^2}{2\alpha}+\frac{k_2^2}{2\beta}\right]\mathrm{e}^{ik\cdot x}\,\mathrm{d}k_1\,\mathrm{d}k_2$$

$$= \frac{(\alpha\beta)^{\frac{1}{2}}}{2\pi}\exp\left[\tfrac{1}{2}(\alpha x^2+\beta y^2)\right] \quad \text{(A 13)}$$

using (A 10). Hence (A 2) is a global attractor for solutions of (A 3) and is therefore the unique stable steady solution in this case. (There may conceivably exist unstable steady solutions that cannot be determined by this method.)

If $\beta>0$, then the form of the exponential factor in (A 12) makes it clear that there is no stable steady solution (with finite non-zero circulation).

Appendix B. Determination of $\psi_{02}(r)$ from solvability condition at $O(\epsilon^3)$

Consideration of terms of order ϵ^3 in (2.7) gives the equation

$$\frac{1}{r}\left[\frac{\partial(\psi_3,\omega_0)}{\partial(r,\theta)}+\frac{\partial(\psi_0,\omega_3)}{\partial(r,\theta)}\right] = -\mathrm{L}_0\omega_2-\lambda\mathrm{L}_1\omega_2-\frac{1}{r}\left[\frac{\partial(\psi_2,\omega_1)}{\partial(r,\theta)}+\frac{\partial(\psi_1,\omega_2)}{\partial(r,\theta)}\right]. \quad \text{(B 1)}$$

Here, ψ_1, ω_1 and ψ_2 are given from (2.32), (2.33), (4.5) by

$$\psi_1 = \lambda f(r)\sin 2\theta, \quad \omega_1 = \lambda\Omega(r)\sin 2\theta, \quad \text{(B 2)}$$

$$\psi_2 = \lambda^2\psi_{02}(r)+\lambda f_2(r)\cos 2\theta+\lambda^2 f_4(r)\cos 4\theta, \quad \text{(B 3)}$$

and we have then also

$$\omega_2 = \lambda^2\Omega_{02}(r)+\lambda\Omega_2(r)\cos 2\theta+\lambda^2\Omega_4(r)\cos 4\theta, \quad \text{(B 4)}$$

where

$$\Omega_{02}(r) = -r^{-1}(r\psi_{02}')', \quad \text{(B 5)}$$

$$\Omega_2(r) = -\mathrm{L}_2 f_2, \quad \Omega_4(r) = -\mathrm{L}_4 f_4. \quad \text{(B 6)}$$

Now the left-hand side of (B 1) (cf. (2.17), (4.1)) may be written as

$$-\frac{1}{r}\frac{\partial}{\partial\theta}(\omega_0'\psi_3+v_0\omega_3). \quad \text{(B 7)}$$

Each term on the right-hand side of (B 1) may be calculated explicitly. The solvability condition is obtained by integrating the equation from $\theta=0$ to $\theta=2\pi$. The left-hand side integrates to zero, and on the right-hand side we get contributions from $-\mathrm{L}_0\Omega_{02}(r)$ and also from terms involving the factor $\cos^2 2\theta$ or $\sin^2 2\theta$. The resulting equation for Ω_{02} is

$$\mathrm{L}_0\Omega_{02} = -r^{-1}S'(r), \quad \text{(B 8)}$$

where

$$S(r) = \tfrac{1}{4}r^2\Omega_2+f_2\Omega-f\Omega_2. \quad \text{(B 9)}$$

The right-hand side of (B 8) is $O(r^2)$ as $r \to 0$, and exponentially small as $r \to \infty$. The function Ω_{02} finite at $r = 0$, exponentially small as $r \to \infty$, and satisfying the normalizing condition

$$\int_0^\infty r\Omega_{02}(r)\,\mathrm{d}r = 0 \tag{B 10}$$

is then given by

$$\Omega_{02}(r) = -\mathrm{e}^{-r^2/4}\int(\mathrm{e}^{r'^2/4}-1)\,S(r')\,r'^{-1}\,\mathrm{d}r'. \tag{B 11}$$

Then, $\psi_{02}(r)$ is given from (B 5) by

$$\psi_{02}(r) = -\int_0^r r'^{-1}\int_0^{r'} r''\Omega_{02}(r'')\,\mathrm{d}r''. \tag{B 12}$$

We see therefore that there is a small modification to the θ-averaged structure of the vortex at $O(\epsilon^2\lambda^2)$.

REFERENCES

BATCHELOR, G. K. 1953 *Homogeneous Turbulence*. Cambridge University Press.

BATCHELOR, G. K. 1956 On steady laminar flow with closed streamlines at large Reynolds number. *J. Fluid Mech.* **1**, 177–190.

BUNTINE, J. D. & PULLIN, D. I. 1989 Merger and cancellation of strained vortices. *J. Fluid Mech.* **205**, 263–295.

DOUADY, S., COUDER, Y. & BRACHET, M. E. 1991 Direct observation of the intermittency of intense vorticity filaments in turbulence. *Phys. Rev. Lett.* **67**, 983–986.

DRITSCHEL, D. G. 1989 Strain induced vortex stripping. In *Mathematical Aspects of Vortex Dynamics* (ed. R. E. Caflisch), pp. 107–119. SIAM.

DRITSCHEL, D. G. 1990 The stability of elliptical vortices in an external straining flow. *J. Fluid Mech.* **210**, 223–261.

HOSOKAWA, I. & YAMAMOTO, K. 1989 Fine structure of a directly simulated isotropic turbulence. *J. Phys. Soc. Japan* **58**, 20–23.

HOSOKAWA, I. & YAMAMOTO, K. 1990 Intermittency of dissipation in directly simulated fully developed turbulence. *J. Phys. Soc. Japan* **59**, 401–404.

JIMÉNEZ, J. 1992 Kinematic alignment effects in turbulent flows. *Phys. Fluids* A **4**, 652–654.

JIMÉNEZ, J., WRAY, A. A., SAFFMAN, P. G. & ROGALLO, R. S. 1993 The structure of intense vorticity in homogeneous isotropic turbulence. *J. Fluid Mech.* **255**, 65–90.

KERR, R. M. 1985 Higher-order derivative correlation and the alignment of small-scale structures in isotropic turbulence. *J. Fluid Mech.* **153**, 31–58.

KIDA, S. 1993 Tube-like structures in turbulence. *Lecture Notes in Numerical Applied Analysis* **12**, 137–159.

KIDA, S. & OHKITANI, K. 1992 Spatio-temporal intermittency and instability of a forced turbulence. *Phys. Fluids* A **4**, 1018–1027 (referred to herein as KO92).

KÜCHEMANN, D. 1965 Report on the IUTAM Symposium on concentrated vortex motions in fluids. *J. Fluid Mech.* **21**, 1–20.

LEGRAS, B. & DRITSCHEL, D. G. 1993 Vortex stripping and the generation of high vorticity gradients in two-dimensional flows. *Appl. Sci. Res.* **51**, 445–455.

LIN, S. J. & CORCOS, G. 1984 The mixing layer: deterministic models of a turbulent flow. Part 3. The effect of plane strain on the dynamics of streamwise vortices. *J. Fluid Mech.* **141**, 139–178.

LINARDATOS, D. 1993 Determination of two-dimensional magnetostatic equilibria and analogous Euler flows. *J. Fluid Mech.* **246**, 569–591.

LUNDGREN, T. 1982 Strained spiral vortex model for turbulent fine structure. *Phys. Fluids* **25**, 2193–2203.

MOFFATT, H. K. 1984 Simple topological aspects of turbulent vorticity dynamics. In *Turbulence and Chaotic Phenomena in Fluids* (ed. T. Tatsumi), pp. 223–230. Elsevier.

MOFFATT, H. K. 1985 Magnetostatic equilibria and analogous Euler flows of arbitrarily complex topology. Part 1. Fundamentals. *J. Fluid Mech.* **159**, 359–378.

MOFFATT, H. K. 1993 Spiral structures in turbulent flow. In *Fractals, Wavelets and Fourier Transforms: New Developments and New Applications* (ed. M. Farge, J. C. R. Hunt & J. C. Vassilicos), pp. 317–324. Clarendon.

NEU, J. C. 1984 The dynamics of stretched vortices. *J. Fluid Mech.* **143**, 253–276.

RHINES, P. B. & YOUNG, W. R. 1982 Homogenization of potential vorticity in planetary gyres. *J. Fluid Mech.* **122**, 347–367.

ROBINSON, A. C. & SAFFMAN, P. G. 1984 Stability and structure of stretched vortices. *Stud. Appl. Maths.* **70**, 163–181.

RUETSCH, G. R. & MAXEY, M. R. 1991 Small scale features of vorticity and passive scalar fields in homogeneous isotropic turbulence. *Phys. Fluids* A **3**, 1587–1597.

SAFFMAN, P. G. 1992 *Vortex Dynamics.* Cambridge University Press.

SAFFMAN, P. G. & BAKER, G. R. 1979 Vortex interactions. *Ann. Rev. Fluid Mech.* **11**, 95–122.

SHE, Z.-S., JACKSON, E. & ORSZAG, S. A. 1990 Intermittent vortex structures in homogeneous isotropic turbulence. *Nature* **344**, 226–228.

SIGGIA, E. D. 1981 Numerical study of small scale intermittency in three-dimensional turbulence. *J. Fluid Mech.* **107**, 375–406.

TANAKA, M. & KIDA, S. 1993 Characterisation of vortex tubes and sheets. *Phys. Fluids* A **5**, 2079–2082.

TENNEKES, H. 1968 Simple model for the small-scale structure of turbulence. *Phys. Fluids.* **11**, 669–671.

TOWNSEND, A. A. 1951 On the fine scale structure of turbulence. *Proc. R. Soc. Lond.* A **208**, 534–542.

VINCENT, A. & MENEGUZZI, M. 1991 The spatial structure and statistical properties of homogeneous turbulence. *J. Fluid Mech.* **225**, 1–25.

YAMAMOTO, K. & HOSOKAWA, I. 1988 A decaying isotropic turbulence pursued by the spectral method. *J. Phys. Soc. Japan* **57**, 1532–1535.